mathematics

MDPI

Article

Memory Effect on Dispersion Process in Hydromagnetic Flows Along a Porous Walls Channel: A Generalized Fick's Flux with Caputo Derivative

N. A. Shah [1], Khalid Masood [2,*] and Dumitru Vieru [3]

[1] Department of Mathematical Sciences, Saveetha School of Engineering, SIMATS, Chennai 602105, Tamil Nadu, India; nashahsaveetha@gmail.com
[2] Department of Mathematics and Statistics, College of Science, Imam Mohammad Ibn Saud Islamic University (IMSIU), Riyadh 11623, Saudi Arabia
[3] Department of Theoretical Mechanics, Technical University of Iasi, 700050 Iasi, Romania; dumitru.vieru@tuiasi.ro
* Correspondence: kmaali@imamu.edu.sa

Abstract

The present study investigates the generalized dispersion of a solute in an incompressible MHD flow via a rectangular channel with injectable or suctioned walls. The mathematical model of dispersion suggests a distinct type of mass flux expressed as a fractional partial differential equation based on the time-fractional Caputo derivative. The mass flow in the model under investigation is determined by both the concentration gradient and its historical evolution. A constant external magnetic field is provided transverse to the flow direction. The analysis and discussion of the analytical solution for the advection velocity are performed in relation to the Hartmann number and the suction/injection Reynolds number. To determine the solute concentration in space and time, the unstable fractional convection–diffusion equation is analytically solved. The polynomial in the geographic variable y that has coefficients that depend on the spatial variable x and the time t is the analytical solution of the concentration. The effects of the fractional order of the Caputo derivative, Reynolds number, Hartmann number, and Peclet number on the advection–diffusion process are examined using numerical simulations of the analytical solution of the solute concentration.

Keywords: generalized dispersion; Caputo derivative; suction and injection; confluent hypergeometric function; Lorenzo–Hartley generalized function

MSC: 76-10; 65M06

Check for updates

Academic Editor: Ramoshweu Solomon Lebelo

Received: 8 November 2025
Revised: 4 December 2025
Accepted: 11 December 2025
Published: 3 February 2026

Copyright: © 2026 by the authors. Licensee MDPI, Basel, Switzerland. This article is an open access article distributed under the terms and conditions of the Creative Commons Attribution (CC BY) license.

1. Introduction

Environmental preservation and the maintenance of air and water quality have long been basic societal goals. It is commonly acknowledged that human well-being is inextricably related to water supply control, emphasizing the need to study the quantitative representation of solute transport in water for exact forecasting of contaminant dispersion. While the conventional advection–dispersion equation has proven effective in delineating solute transportation mechanisms, studies of tracer movement at various scales have revealed instances where the traditional advection–diffusion model fails to accurately depict certain transport phenomena. Such cases of transport have been classified as anomalous or non-Fickian [1].

Modern fractional calculus has shown to be an excellent technique for defining solute mobility that is not Fickian. Nonlocal models, or mathematical models based on fractional differential operators, are commonly used to simulate non-Fickian transport phenomena. Various studies have found that fractional advection–diffusion equations are a more effective way to portray the behavior of pollutants in a controllable manner (see [2,3]). Benson et al. [4] reported two significant studies demonstrating non-Fickian mass transfer characteristics, which provided information on the breadth and speed of tracer mobility. Povstenko [5] found the fundamental solutions to the fractional two-dimensional advection–diffusion equation, with and without a base. The characteristics of these fundamental solutions, as well as their theoretical and practical ramifications, were highlighted. Jiang and Lin [6] developed a very effective numerical approach for solving the equations for time–space fractional advection–dispersion with variable coefficients inside a limited domain. The investigated fractional differential equation includes the fractional Riemann–Liouville and Caputo derivatives. Nasrudin et al. [7] developed a numerical technique for solving fractal–fractional advection–diffusion-reaction equations by combining the Ritz approximation method with a satisfier function. Wang et al. [8] presented a thorough mathematical description for the nonlocal transport features of silt particles in ice-covered channels that flow consistently and steadily. Their model predicts the vertical diffusion of scattered sediment particles in such channels using a fractional advection–dispersion equation and the Caputo fractional derivative.

The results show that the fractional derivative approach outperforms real data in terms of predicting suspended sediment concentrations. Qiao et al. [9] used a time fractional advection–dispersion equation to investigate chloride ion migration in a single vertical fracture in several rough-wall scenarios. A comparison of FADE solutions with the standard advection–dispersion equation was performed, demonstrating that the fractional model is superior in understanding solute transport processes in fractures, especially at low flow rates and high roughness conditions. Grant and Wilkinson [10] studied a uniform advection–diffusion equation (ADE) with a time-dependent drift velocity and diffusion tensor for totally permeable and absorbing barrier situations. Wang and Barkai [11] explored a fractional advection–diffusion equation that describes distribution packets to elucidate transport mechanisms in disordered systems. In contrast to conventional transport mechanisms involving diffusion and drift, their study unveiled a third term indicating symmetry breaking as a prevalent factor in disordered system transport phenomena. Das et al. [12] investigated the impact of suction/injection on Fickian transport within a rectangular channel featuring reactive porous boundaries. They derived a semi-analytical solution for solute concentration, and determined the dispersion coefficient, skewness, and kurtosis of solute distribution over time. Hristov [13] conducted a thorough and well-structured examination of non-local kinetic models, emphasizing the uses of fractional calculus. This investigation elucidates the utility of power-law kinetics; fractional operators' dependence upon it; memories derived from non-singular Mittag–Leffler kernels; and diffusion models incorporating fractional operators that are non-singular, like Atangana–Baleanu and derivatives, in elucidating intricate transport phenomena. Vieru et al. [14] introduced generalized fractional operators within Mittag–Leffler memory kernels, added to their associated properties. They further established a generalized mathematical framework for advection–dispersion processes in addition to kinetic adsorption by integrating the diffusive flow equation featuring the new generalized time-fractional derivative. The authors subsequently derived analytical solutions for the generalized equation of advection–dispersion with kinetic adsorption by utilizing the Laplace transform method.

Human activities can sometimes be harmful to the environment and can lead to air and water pollution. Knowledge of the dispersion process of pollutants is essential for environ-

mental conservation and for maintaining air and water quality. These essential desires have led researchers to extensively approach the study of dispersion advection processes. Following the same line, in this article we investigate generalized advection-dispersion processes suitable for providing new and interesting information about the transport mechanisms of polluting substances in fluid media.

More precisely, the objective of the current study is to examine the generalized dispersion of solute phenomenon in an incompressible MHD flow within a rectangular channel featuring suction/injection on the boundaries. A novel mathematical framework for the dispersion is introduced, where the mass flux is governed by a fractional PDE utilizing the time-fractional Caputo derivative. This model accounts for the mass flux being influenced not solely by the concentration gradient but also by its prior action. The fluid dynamics are impacted by a constant external magnetic field perpendicular to the flow direction. The advection velocity's analytical solution is derived and deliberated with regard to the suction/injection Reynolds number and the Hartmann number. Subsequently, the transient fractional convection–diffusion equation is worked out numerically to determine the solute concentration across space and time. The concentration's analytical solution is represented as a polynomial in the spatial variable y, with coefficients being functions reliant on the spatial variable x and the time t. These coefficients are expressed using the confluent hypergeometric and the generalized G–Lorenzo–Hartley functions. Utilizing numerical simulations, the impact of the fractional order of the Caputo derivative, Reynolds number, Hartmann number, and Peclet number on the generalized advection-diffusion process is scrutinized.

2. Mathematical Formulation of the Problem

Let us consider the one-dimensional flow of an electrically conducting viscous fluid in a rectangular channel bounded by two infinite permeable parallel plates located in the planes $Y = 0$ and $Y = H$, respectively, of the Cartesian coordinate system $0XYZ$ (see Figure 1).

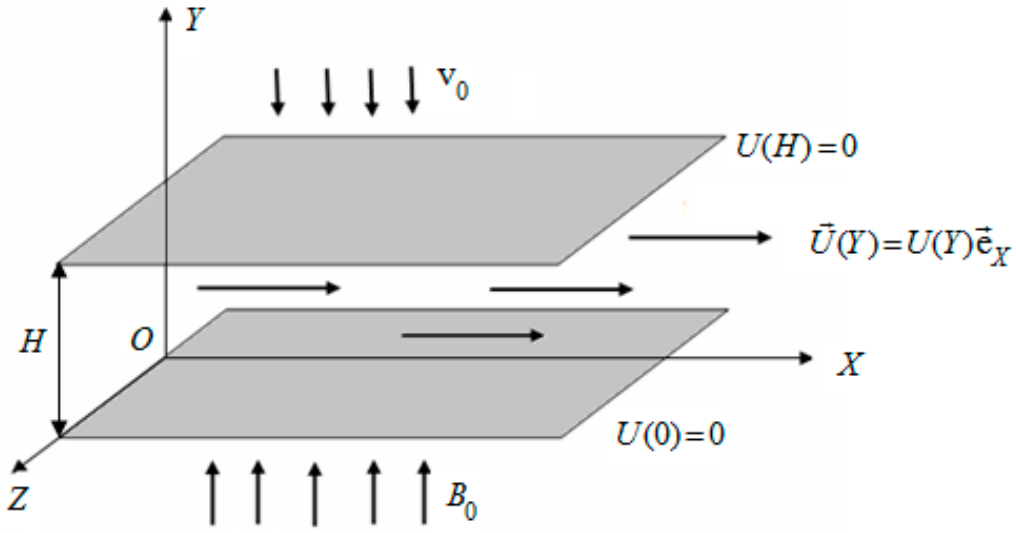

Figure 1. Schematic flow geometry.

The fluid motion is influenced by an external magnetic field of constant intensity B_0 that acts perpendicularly on the channel walls. The characteristic suction/injection constant velocity v_0 is supposed to be directed perpendicular to the fluid flow and it guarantees stationary flow with the pressure gradient in the flow direction, $\frac{\partial P}{\partial X} = P_0 \cos\left(\frac{(2Y-H)\pi}{2H}\right)$.

The governing equation of the fluid motion is [12]

$$\mu \frac{d^2U(Y)}{dY^2} - \rho v_0 \frac{dU(Y)}{dY} - \sigma B_0^2 U(Y) = \frac{\partial P(X,Y)}{\partial X}, \tag{1}$$

where μ is the viscosity of fluid, ρ is the density of fluid, and σ is the electrical conductivity of the fluid. $\vec{U}(Y) = U(Y)\vec{e}_X$ is the fluid velocity, and $\vec{e}_X$ is the unit vector of the X-axis.

Introducing the non-dimensional quantities

$$x = \frac{X}{H}, \ y = \frac{Y}{H}, \ Re = \frac{v_0 H}{\nu}, \ u = \frac{U}{u_0}, \ \mathrm{Ha}^2 = \frac{\sigma}{\mu} B_0^2 H^2, \ \nu = \frac{\mu}{\rho}, \ u_0 = \frac{P_0 H^2}{\rho \nu}, \tag{2}$$

we acquire the non-dimensional form of Equation (1) as follows:

$$\frac{d^2u(y)}{dy^2} - \mathrm{Re}\frac{du(y)}{dy} - Ha^2 u(y) = \sin(\pi y), \ y \in [0,1]. \tag{3}$$

In the above equation, Re is the Reynolds number, Ha is the Hartmann number, and the spatial nondimensional variable y.

Along with Equation (3), the following no-slip boundary conditions are considered:

$$u(0) = 0, \quad u(1) = 0. \tag{4}$$

Now, let us consider a tracer that is passive with uniform molecular diffusion D that is openly available in the steady flow described by Equation (3). We denote by $C(X,Y,T)$ the solute concentration and by $\vec{J}$ the diffusion flux. The above equations obey Fick's laws [14,15], as follows:

The convection–diffusion equation without sources.

$$\frac{\partial C}{\partial T} + \nabla \cdot \vec{J} = 0; \tag{5}$$

The diffusion flux

$$\vec{J}_1 = -D\nabla C; \tag{6}$$

The current density of the quantity C

$$\vec{J} = \vec{J}_1 + C\vec{U}, \tag{7}$$

$\vec{U}$ being the drift velocity. In these equations, T denotes the dimensional time and the term $C\vec{U}$ describes the convection (or advection). Using the dimensionless parameters given by Equation (2), together with

$$t = \frac{DT}{H^2}, \ \phi = \frac{C}{C_0}, \ \vec{\mathrm{j}}_1 = \frac{H\vec{J}_1}{C_0 D}, \ \vec{\mathrm{j}} = \frac{H\vec{J}}{C_0 D}, \ Pe = \frac{Hu_0}{D}, \tag{8}$$

where C_0 is a characteristics concentration, Equations (5)–(7) become

$$\frac{\partial \phi(x,y,t)}{\partial t} + \nabla \cdot \vec{j}(x,y,t) = 0, \tag{9}$$

$$\vec{j}_1(x,y,t) = -\nabla\phi(x,y,t), \tag{10}$$

$$\vec{j}(x,y,t) = \vec{j}_1(x,y,t) + \mathrm{P}_e \vec{u}(y)\phi(x,y,t). \tag{11}$$

Equations (9)–(11) imply that in the non-dimensional concentration $\phi(x,y,t)$.

$$\frac{\partial \phi}{\partial t} + \mathrm{P}_e u(y)\frac{\partial \phi}{\partial x} = \frac{\partial^2 \phi}{\partial x^2} + \frac{\partial^2 \phi}{\partial y^2}. \tag{12}$$

For the solute dimensionless concentration $\phi(x,y,t)$, we suppose the initial boundary conditions

$$\phi(x,y,0) = 0, \quad x \in \mathbb{R}, \quad y \in [0,1], \tag{13}$$

$$\left.\frac{\partial \phi(x,y,t)}{\partial y}\right|_{y=0} = t^k e^{-x^2 t}, \ \mathrm{k} \geq 2, \ x \in \mathbb{R}, \ \ t > 0, \tag{14}$$

$$\lim_{|x|\to\infty} \phi(x,y,t) = 0, \quad y \in [0,1], \quad t \geq 0. \tag{15}$$

The Generalized Fractional Convection–Diffusion Process

In this section we formulate a generalized mathematical structure of the convection–diffusion transport based on the generalized fractional Fick's law [16], namely

$$\vec{j}_{\,1}(x,y,t) = -{}^{C}D_t^{1-\alpha}[\nabla \phi(x,y,t)], \quad 0 < \alpha \leq 1, \tag{16}$$

where

$${}^{C}D_t^{\alpha}\chi(x,y,t) = \begin{cases} \dfrac{1}{\Gamma(1-\alpha)}\displaystyle\int_0^t (t-\tau)^{-\alpha}\frac{\partial \chi(x,y,\tau)}{\partial \tau}d\tau, \ \ 0 < \alpha < 1, \\ \dfrac{\partial^{\alpha}\chi(x,y,t)}{\partial t^{\alpha}}, \ \ \alpha \in \{0,1\}, \end{cases} \tag{17}$$

is the Caputo time-fractional derivative of order α [17,18].

Making $\alpha = 1$ in Equation (16), the ordinary Fick's law (10) is obtained.

The non-dimensional current density of the non-dimensional concentration becomes

$$\vec{j}\,(x,y,t) = -{}^{C}D_t^{1-\alpha}[\nabla \phi(x,y,t)] + \mathrm{P}_e \vec{u}\,(y)\phi(x,y,t). \tag{18}$$

Using (18) in Equation (9), we obtain that the non-dimensional concentration $\phi(x,y,t)$ has to satisfy the generalized convection–diffusion equation.

$$\frac{\partial \phi}{\partial t} + \mathrm{P}_e u(y)\frac{\partial \phi}{\partial x} = {}^{C}D_t^{1-\alpha}\left[\frac{\partial^2 \phi}{\partial x^2} + \frac{\partial^2 \phi}{\partial y^2}\right], \tag{19}$$

along with the initial and boundary conditions (13)–(15).

3. Analytical Solution for the Velocity Field $u(y)$

The velocity field $u(y)$ is the solution for the DE (3), along with the boundary conditions (4).

A particular solution of Equation (3) is given by

$$u_p(y) = A\sin(\pi y) + B\cos(\pi y) \tag{20}$$

where

$$A = -\frac{Ha^2 + \pi^2}{(Ha^2+\pi^2)^2 + (Re\pi)^2}, \ \mathrm{B} = \frac{Re\pi}{(Ha^2+\pi^2)^2 + (Re\pi)^2}. \tag{21}$$

The general solution of Equation (3) is

$$u(y) = \left[C_1\cosh\left(\frac{y}{2}\sqrt{\mathrm{Re}^2 + 4Ha^2}\right) + C_2\sinh\left(\frac{y}{2}\sqrt{\mathrm{Re}^2 + 4Ha^2}\right)\right]\exp\left(\frac{Rey}{2}\right) + u_p(y) \tag{22}$$

where C_1 and C_2 are the integration constants. Using boundary conditions (4), we obtain the following values of the constants C_1 and C_2:

$$C_1 = -B; \quad C_2 = \frac{\exp\left(-\frac{Re}{2}\right) + \cosh\left(\frac{1}{2}\sqrt{Re^2 + 4Ha^2}\right)}{\sinh\left(\frac{1}{2}\sqrt{Re^2 + 4Ha^2}\right)} B. \tag{23}$$

Using the Taylor series, the velocity field in Equation (22) can be written in the equivalent form

$$u(y) = \sum_{k=1}^{\infty} \left(p_{2k-1} y^{2k-1} + p_{2k} y^{2k}\right) = p_1 y + p_2 y^2 + p_3 y^3 + \ldots = \sum_{n=1}^{\infty} p_n y^n, \tag{24}$$

where

$$\left.\begin{array}{l} p_{2k-1} = \frac{1}{(2k-1)!}\left[\frac{C_1+C_2}{2} a_1^{2k-1} + \frac{C_1-C_2}{2} a_2^{2k-1} - (-1)^k A\pi^{2k-1}\right], \ k = 1, 2, \ldots \\ p_{2k} = \frac{1}{(2k)!}\left[\frac{C_1+C_2}{2} a_1^{2k} + \frac{C_1-C_2}{2} a_2^{2k} + (-1)^k B\pi^{2k}\right], \ k = 1, 2, \ldots \\ a_1 = \frac{1}{2}\left(Re + \sqrt{Re^2 + 4Ha^2}\right), \ a_2 = \frac{1}{2}\left(Re - \sqrt{Re^2 + 4Ha^2}\right). \end{array}\right\} \tag{25}$$

Figures 2 and 3 show velocity curves for different Reynolds and Hartmann numbers. Figure 2 shows the velocity distribution for various Reynolds number values. The Reynolds number positive values represent suction through the channel walls, whereas negative Reynolds numbers relate to the injection process. It is noticed that the suction process increases fluid velocity in the direction of the top wall, but the injection Reynolds number increases fluid velocity across the bottom wall. It should also be observed that the highest fluid velocity occurs in the area closer to the top wall in the event of suction, and in the area closer to the lower wall for injection. The highest velocity value is achieved in the case of impermeable walls when the Reynolds number is equal to zero.

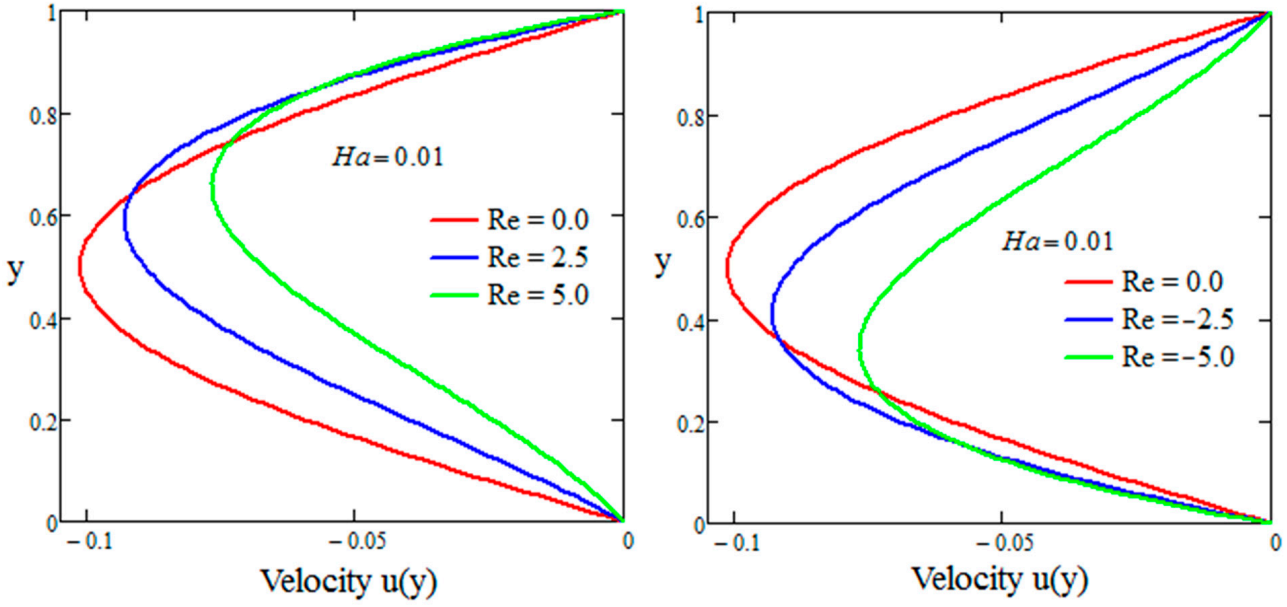

Figure 2. Velocity profiles for various values of the Reynolds number and for Hartmann number Ha = 0.01.

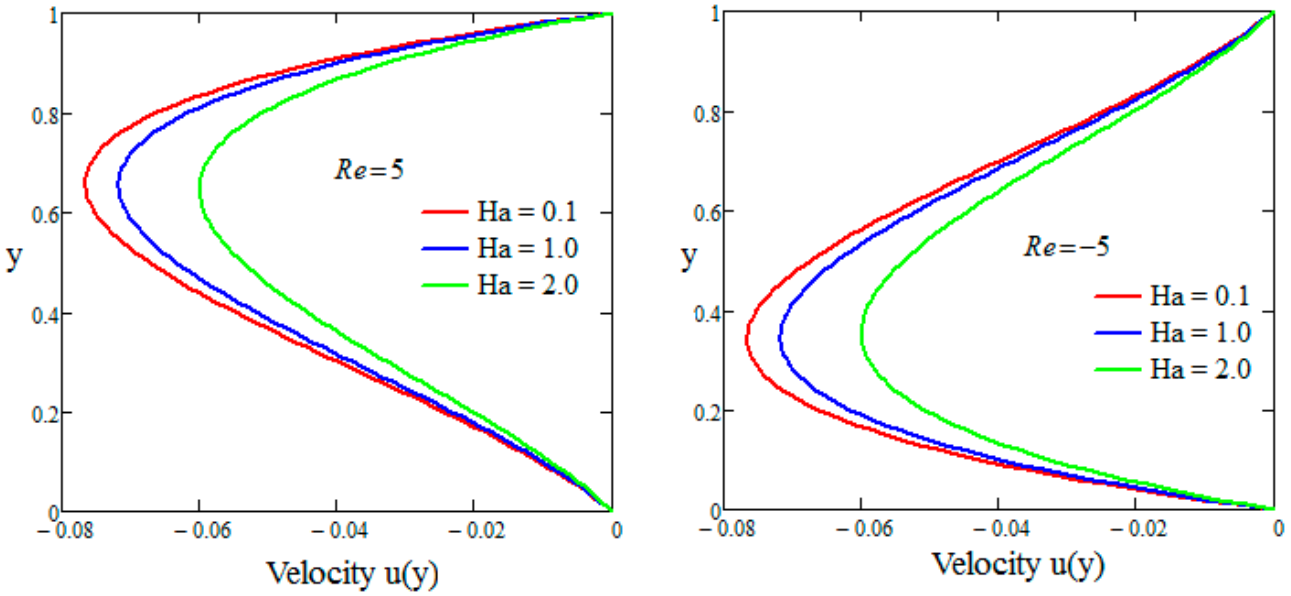

Figure 3. Velocity profiles for various values of the Hartmann number and for Reynolds number $\mathrm{Re} = \pm 5$.

Figure 3 presents the velocity profiles corresponding to three different Hartmann numbers and two distinct Reynolds numbers, namely, $\mathrm{Re} = \pm 5$. It is perceived that as the Hartmann number Ha improves, the velocity prominently decreases. This behavior is due to the presence of the Lorentz force, which acts as a force that slows down the movement of the fluid.

4. Analytical Solution for the Concentration $\phi(x, y, t)$

The concentration field $\phi(x, y, t)$ is the solution of the fractional partial differential Equation (19), in addition to the initial and boundary conditions (13)–(15).

Considering expression (24) of the velocity field, we will look for the solution of Equation (19) in the form

$$\phi(x, y, t) = \sum_{n=1}^{\infty} \varphi_n(x, t) y^n, \quad x \in \mathbb{R}, \quad t \geq 0, \quad y \in [0, 1] \tag{26}$$

Substituting (26) into Equation (19), we obtain the following relationship:

$$\sum_{n=1}^{\infty} \frac{\partial \varphi_n}{\partial t} y^n + \sum_{n=1}^{\infty} \left(P_e \sum_{k=1}^{n} p_k \frac{\partial \varphi_{n-k+1}}{\partial x} \right) y^n = \sum_{n=1}^{\infty} {}^{C}D_t^{1-\alpha} \left[\frac{\partial^2 \varphi_n}{\partial x^2} + (n+1)(n+2)\varphi_{n+2} \right] y^n + \\ + 2\,{}^{C}D_t^{1-\alpha} \varphi_2(x, t). \tag{27}$$

Identifying the coefficients of the y^n, $n = 1, 2, \ldots$, we find that functions $\varphi_n(x, t)$ have to satisfy the equations

$$\varphi_2(x, t) = 0, \tag{28}$$

$$\frac{\partial \varphi_n(x, t)}{\partial t} + P_e \sum_{k=1}^{n} p_k \frac{\partial \varphi_{n-k+1}(x, t)}{\partial x} = {}^{C}D_t^{1-\alpha} \left[\frac{\partial^2 \varphi_n(x, t)}{\partial x^2} + (n+1)(n+2)\varphi_{n+2}(x, t) \right], \quad n = 1, 2, \ldots \tag{29}$$

Using initial and boundary conditions (13)–(15), we find that the functions $\varphi_n(x, s)$ have to satisfy the following conditions

$$\varphi_n(x, 0) = 0, \quad n = 1, 2, \ldots \tag{30}$$

$$\varphi_1(x,t) = t^k e^{-x^2 t},\ k \geq 2,\ x \in \mathbb{R},\ t \geq 0 \tag{31}$$

$$\lim_{|x|\to\infty} \varphi_n(x,t) = 0, \quad n = 1,2,\ldots \tag{32}$$

Applying the fractional integral operator [14,19]

$$I_t^{1-\alpha}\chi(x,y,t) = \begin{cases} \frac{1}{\Gamma(1-\alpha)}\int_0^t (t-\tau)^{-\alpha}\chi(x,y,\tau)d\tau, & 0 \leq \alpha < 1, \\ \chi(x,y,t), & \alpha = 1 \end{cases} \tag{33}$$

to Equation (29) and using the properties

$$\begin{aligned} &I_t^{1-\alpha}\left(\tfrac{\partial\chi(x,y,t)}{\partial t}\right) = {}^C D_t^\alpha \chi(x,y,t), \\ &I_t^{1-\alpha}\left({}_C D_t^{1-\alpha}\chi(x,y,t)\right) = \chi(x,y,t),\ \text{if } \chi(x,y,0) = 0 \end{aligned} \tag{34}$$

we find that the functions $\varphi_n(x,s)$ are solutions of the fractional differential equation

$${}^C D_t^\alpha \varphi_n(x,t) + P_e \sum_{k=1}^{n} p_k \frac{\partial}{\partial x}\left[I_t^{1-\alpha}\varphi_{n-k+1}(x,t)\right] = \frac{\partial^2\varphi_n(x,t)}{\partial x^2} + (n+1)(n+2)\varphi_{n+2}(x,t),\ \ n = 1,2,\ldots \tag{35}$$

The recurrence relation (35) determines the functions $\varphi_3(x,t),\ \varphi_4(x,t),\ldots$. Making $n = 1$ in Equation (35), we obtain

$$6\varphi_3(x,t) = {}^C D_t^\alpha \varphi_1(x,t) + P_e p_1 I_t^{1-\alpha}\left(\frac{\partial\varphi_1(x,t)}{\partial x}\right) - \frac{\partial^2\varphi_1(x,t)}{\partial x^2} \tag{36}$$

Using (17), (31), and (34), we obtain

$${}^C D_t^\alpha \varphi_1(x,t) = \frac{1}{\Gamma(1-\alpha)}\int_0^t (t-\tau)^{-\alpha}\frac{\partial\varphi_1(x,\tau)}{\partial\tau}d\tau = \frac{1}{\Gamma(1-\alpha)}\int_0^t (t-\tau)^{-\alpha}(k\tau^{k-1} - x^2\tau^k)e^{-x^2\tau}d\tau \tag{37}$$

Let us recall the following integral [20]:

$$\int_0^u (u-x)^{\mu-1}x^{v-1}e^{\beta x}dx = B(\mu,v)u^{\mu+v-1}{}_1F_1(v;\mu+v;\beta u), \tag{38}$$

where $\mathrm{Re}\mu > 0, \mathrm{Re}v > 0,$ and $B(\mu,\nu)$ is Euler's integral of the first kind, defined as [20]

$$B(\mu,v) = \int_0^1 t^{\mu-1}(1-t)^{v-1}dt, \tag{39}$$

Function ${}_1F_1(\alpha;\gamma;z)$ is the degenerate hypergeometric function (also called confluent hypergeometric function) given by [21]

$$\begin{aligned} {}_1F_1(\alpha;\gamma;z) &= 1 + \tfrac{\alpha}{\gamma}\tfrac{z}{1!} + \tfrac{\alpha(\alpha+1)}{\gamma(\gamma+1)}\tfrac{z^2}{2!} + \tfrac{\alpha(\alpha+1)(\alpha+2)}{\gamma(\gamma+1)(\gamma+2)}\tfrac{z^3}{3!} + \ldots \\ &= \tfrac{z^{1-\gamma}}{B(\alpha,\gamma-\alpha)}\int_0^z e^t t^{\alpha-1}(z-t)^{\gamma-\alpha-1}dt. \end{aligned} \tag{40}$$

Using (38), Equation (37) becomes

$$
\begin{aligned}
&{}^{C}D_t^{\alpha}\varphi_1(x,t) = \frac{1}{\Gamma(1-\alpha)}\int_0^t (t-\tau)^{(1-\alpha)-1}\left[k\tau^{k-1} - x^2\tau^{(k+1)-1}\right]e^{-x^2\tau}d\tau = \\
&\frac{kB(1-\alpha,k)t^{k-\alpha}}{\Gamma(1-\alpha)}{}_1F_1(k;k+1-\alpha;-x^2t) - \frac{x^2t^{k+1-\alpha}B(1-\alpha,k+1)}{\Gamma(1-\alpha)}{}_1F_1(k+1;k+2-\alpha;-x^2t) = \\
&\frac{k\Gamma(k)t^{k-\alpha}}{\Gamma(k+1-\alpha)}{}_1F_1(k;k+1-\alpha;-x^2t) - \frac{x^2t^{k+1-\alpha}\Gamma(k+1)}{\Gamma(k+2-\alpha)}{}_1F_1(k+1;k+2-\alpha;-x^2t).
\end{aligned} \tag{41}
$$

In the same way, we obtain

$$
\begin{aligned}
&I_t^{1-\alpha}\left(\frac{\partial\varphi_1(x,t)}{\partial x}\right) = \frac{1}{\Gamma(1-\alpha)}\int_0^t (t-\tau)^{-\alpha}(-2x\tau^{k+1})\exp(-x^2\tau)d\tau = \\
&\frac{-2x}{\Gamma(1-\alpha)}\int_0^t (t-\tau)^{(1-\alpha)-1}\tau^{(k+2)-1}e^{-x^2\tau}d\tau = \frac{-2x}{\Gamma(1-\alpha)}B(1-\alpha,k+2)t^{k+2-\alpha}{}_1F_1(k+2;k+3-\alpha;-x^2t) = \\
&\frac{-2xt^{k+2-\alpha}\Gamma(k+2)}{\Gamma(k+3-\alpha)}{}_1F_1(k+2;k+3-\alpha;-x^2t).
\end{aligned} \tag{42}
$$

On the other hand, from (31) we obtain

$$
\frac{\partial\varphi_1}{\partial x} = -2xt^{k+1}e^{-x^2t}; \frac{\partial^2\varphi_1}{\partial x^2} = 2t^{k+1}(2x^2t-1)e^{-x^2t} \tag{43}
$$

Substituting (41)–(43) into Equation (36), we obtain

$$
\begin{aligned}
&\varphi_3(x,t) = \tfrac{t^{k+1}(1-2tx^2)}{3}e^{-tx^2} + \tfrac{k\Gamma(k)t^{k-\alpha}}{6\Gamma(k+1-\alpha)}{}_1F_1(k;k+1-\alpha;-x^2t) - \\
&\tfrac{x^2t^{k+1-\alpha}\Gamma(k+1)}{6\Gamma(k+2-\alpha)}{}_1F_1(k+1;k+2-\alpha;-x^2t) - \tfrac{Pep_1}{3}\tfrac{xt^{k+2-\alpha}\Gamma(k+2)}{\Gamma(k+3-\alpha)}{}_1F_1(k+2;k+3-\alpha;-x^2t).
\end{aligned} \tag{44}
$$

In the particular case $\alpha = 1$, Equation (36) becomes

$$
\begin{aligned}
\varphi_3 = \tfrac{1}{6}\left[\tfrac{\partial\varphi_1}{\partial t} + P_ep_1\tfrac{\partial\varphi_1}{\partial x} - \tfrac{\partial^2\varphi_1}{\partial x^2}\right] &= \tfrac{1}{6}\left[t^{k-1}(k-x^2t)e^{-x^2t} - 2P_ep_1xt^{k+1}e^{-x^2t} + 2t^{k+1}(1-2x^2t)e^{-x^2t}\right] \\
&= \tfrac{t^{k-1}}{6}\left[k - x^2t(1+4t^2) + 2t^2(1-P_ep_1x)\right]e^{-x^2t}.
\end{aligned} \tag{45}
$$

Let us show that Equation (44) is equivalent to (45) for $\alpha = 1$. Indeed, using the property

$$
{}_1F_1(a;a;-x^2t) = 1 + \frac{(-x^2t)}{1!} + \frac{(-x^2t)^2}{2!} + \ldots = e^{-x^2t}, \tag{46}
$$

for $\alpha = 1$, Equation (44) leads to

$$
\begin{aligned}
&\varphi_3(x,t) = \tfrac{t^{k+1}(1-2tx^2)}{3}e^{-tx^2} + \tfrac{kt^{k-1}}{6}e^{-tx^2} - \tfrac{x^2t^k}{6}e^{-tx^2} - \tfrac{Pep_1xt^{k+1}}{3}e^{-tx^2} = \\
&\tfrac{t^{k-1}}{6}\left[k - x^2t(1+4t^2) + 2t^2(1-P_ep_1x)\right]e^{-x^2t},
\end{aligned}
$$

therefore, (45) is recovered.

It is clear that the function $\varphi_1(x,t)$ given by (31) satisfies conditions (30) and (32). Also, the property $\lim\limits_{t\to\infty}\varphi_1(x,t) = 0,\ for\ k \geq 2,\ x \in \mathbb{R}$ is evident. Let us show that the function $\varphi_3(x,t)$ satisfies properties (30) and (32).

Making $t = 0$ in Equation (44) and using the equality ${}_1F_1(\alpha;\gamma;0) = 1$, we obtain $\varphi_3(x,0) = 0, for\ k \geq 2,\ x \in \mathbb{R},\ \alpha \in [0,1]$. Now, let us prove the following lemma:

Lemma 1. *Function $\varphi_3(x,t)$ satisfies the following properties:*

$$
\text{(a)}\ \lim_{|x|\to\infty}\varphi_3(x,t) = 0,\ for\ t \geq 0,\ \alpha \in [0,1], \tag{47}
$$

$$\text{(b)}\ \lim_{t\to\infty}\varphi_3(x,t)=0,\ for\ x\in\mathbb{R},\ \alpha\in[0,1]. \tag{48}$$

Proof. Let $\overline{\phi}_1(x,s)=L\{\exp(-x^2t)\}=\int_0^\infty \exp(-x^2t)\exp(-st)dt=\frac{1}{s+x^2}$ be the Laplace transform of the function $\exp(-x^2t)$. Using the properties of the Laplace transforms [22,23], we determine that

$$\overline{\varphi}_1(x,s)=L\{\varphi_1(x,t)\}=L\left\{t^k\exp(-x^2t)\right\}=(-1)^k\frac{d^k\overline{\phi}_1}{ds^k}=\frac{k!}{(s+x^2)^{k+1}} \tag{49}$$

Using Equation (36), we obtain the Laplace transform of the function $\varphi_3(x,t)$ as

$$\overline{\varphi}_3(x,s)=\frac{1}{6}\left[s^\alpha\overline{\varphi}_1(x,s)+Pep_1s^{\alpha-1}\frac{\partial\overline{\varphi}_1(x,s)}{\partial x}-\frac{\partial^2\overline{\varphi}_1(x,s)}{\partial x^2}\right] \tag{50}$$

Using (49), Equation (50) becomes

$$\overline{\varphi}_3(x,s)=\frac{1}{6}\left[\frac{k!s^\alpha}{(s+x^2)^{k+1}}+\frac{2(k+1)![1-Pep_1xs^{\alpha-1}]}{(s+x^2)^{k+2}}-\frac{4x^2(k+2)!}{(s+x^2)^{k+3}}\right] \tag{51}$$

Now, we obtain $\lim_{|x|\to\infty}\varphi_3(x,t)=\lim_{|x|\to\infty}\overline{\varphi}_3(x,s)=0$, $\lim_{t\to\infty}\varphi_3(x,t)=\lim_{s\to0}s\overline{\varphi}_3(x,s)=0$, so, the statements in Lemma 1 are true. □

We now present other expressions of the functions $\varphi_1(x,t)$ and $\varphi_3(x,t)$, equivalent to (31) and (44), respectively, using the generalized Lorenzo–Hartley functions defined as follows [24]:

$$G_{a,b.c}(t,d)=L^{-1}\left\{\frac{s^b}{(s^a+d)^c}\right\},\ \mathrm{Re}(ac-b)>0,\ \mathrm{Re}(s)>0,\ |d|<|s^a| \tag{52}$$

$$G_{a,b.c}(t,d)=\sum_{j=0}^{\infty}\frac{(-d)^j\Gamma(c+j)}{\Gamma(c)\Gamma(j+1)\Gamma((c+j)a-b))}t^{(c+j)a-b-1} \tag{53}$$

Using (52) in (49) and (51), we have

$$\begin{array}{l}\varphi_1(x,t)=G_{1,0,k+1}(t,x^2),\\ \varphi_3(x,t)=\frac{1}{6}\left[k!G_{1,\alpha,k+1}(t,-x^2)+2(k+1)!G_{1,0,k+2}(t,-x^2)-\right.\\ \left.2(k+1)!Pep_1xG_{1,\alpha-1,k+2}(t,-x^2)-4x^2(k+2)!G_{1,0,k+3}(t,-x^2)\right].\end{array} \tag{54}$$

To determine functions $\varphi_n(x,t)$, $n\geq4$, it is advantageous to use the Laplace transform. Utilizing the Laplace transform to Equation (35), we obtain

$$(n+1)(n+2)\overline{\varphi}_{n+2}(x,s)=s^\alpha\overline{\varphi}_n(x,s)+Pe\sum_{k=1}^{n}p_ks^{\alpha-1}\frac{\partial\overline{\varphi}_{n-k+1}(x,s)}{\partial x}-\frac{\partial^2\overline{\varphi}_n(x,s)}{\partial x^2},\ n\geq2 \tag{55}$$

Making $n=2$ in Equation (55), we obtain the Laplace transform of the function $\varphi_4(x,t)$ as

$$\overline{\varphi}_4(x,s)=\frac{-Pep_2(k+1)!xs^{\alpha-1}}{6(s+x^2)^{k+2}}. \tag{56}$$

The inverse Laplace transform of the function (56) is

$$\varphi_4(x,t)=\frac{-Pep_2(k+1)!x}{6}G_{1,\alpha-1,k+2}(t,-x^2) \tag{57}$$

The function $\varphi_4(x,t)$ has the following properties:

$$\lim_{t\to 0}\varphi_4(x,t)=\lim_{s\to\infty}s\overline{\varphi}_4(x,s)=0;\ \lim_{t\to\infty}\varphi_4(x,t)=\lim_{s\to 0}s\overline{\varphi}_4(x,s)=0;\ \lim_{|x|\to\infty}\varphi_4(x,t)=\lim_{|x|\to\infty}\overline{\varphi}_4(x,s)=0. \quad (58)$$

In the particular case $\alpha=1$, function (57) becomes $\varphi_4(x,t)=\frac{-Pep_2(k+1)xt^{k+1}}{6}e^{-x_2t}$.

Continuing the recurrent procedure given by Equation (56), other functions $\varphi_n(x,t)$, $n\geq 5$ can be determined. Taking into account the fact that $y\in[0,1]$, we will discuss the approximate analytical solution that contains the powers of $y^n, n\leq 4$, namely the solution

$$\phi(x,y,t)=\sum_{n=1}^{4}\varphi_n(x,t)y^n,\ \ x\in\mathbb{R},\ \ t\geq 0,\ \ y\in[0,1] \quad (59)$$

5. Results and Discussions

The analytical expression of the nondimensional solute concentration is used for the numerical simulation of the diffusion process. The numerical results and graphical illustrations of the concentration profiles were obtained using the Mathcad 15 software. Graphs in Figures 4–7 show the concentration profiles at different moments in time, in different vertical positions in the channel, and for different intervals of variation in the longitudinal variable x. In particular, the impact of the memory α parameter on the solute diffusion process was highlighted.

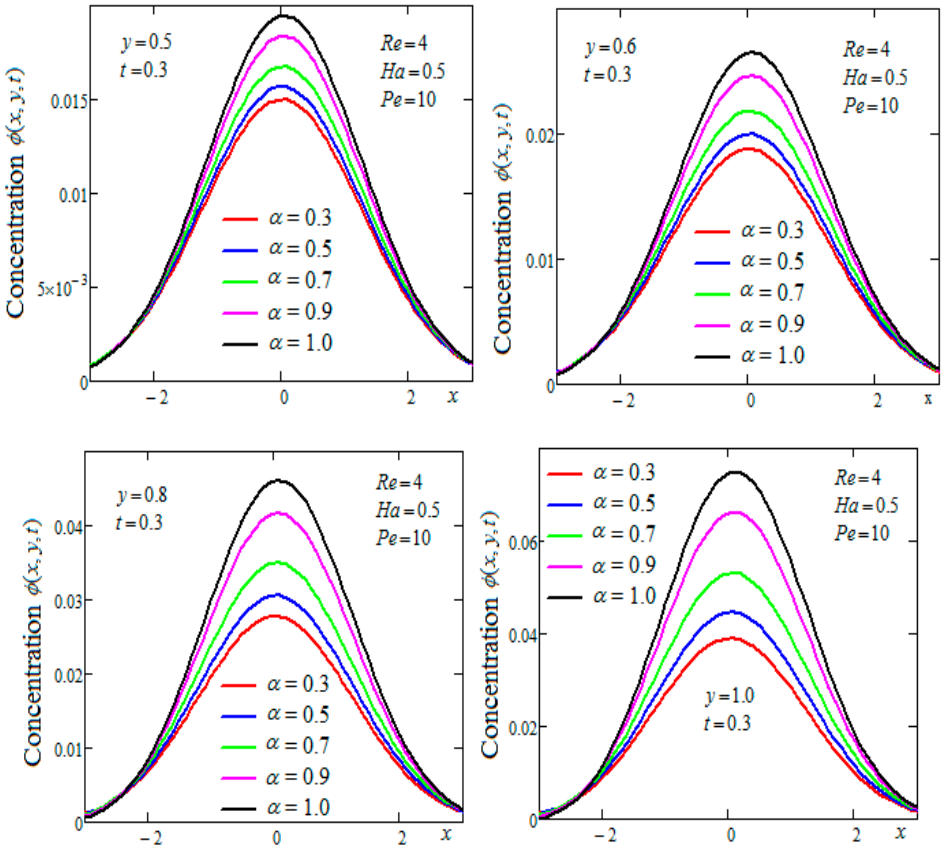

Figure 4. Profiles of the concentration $\phi(x,y,t)$ for various values of the vertical position of the channel and with varying the fractional parameter α values.

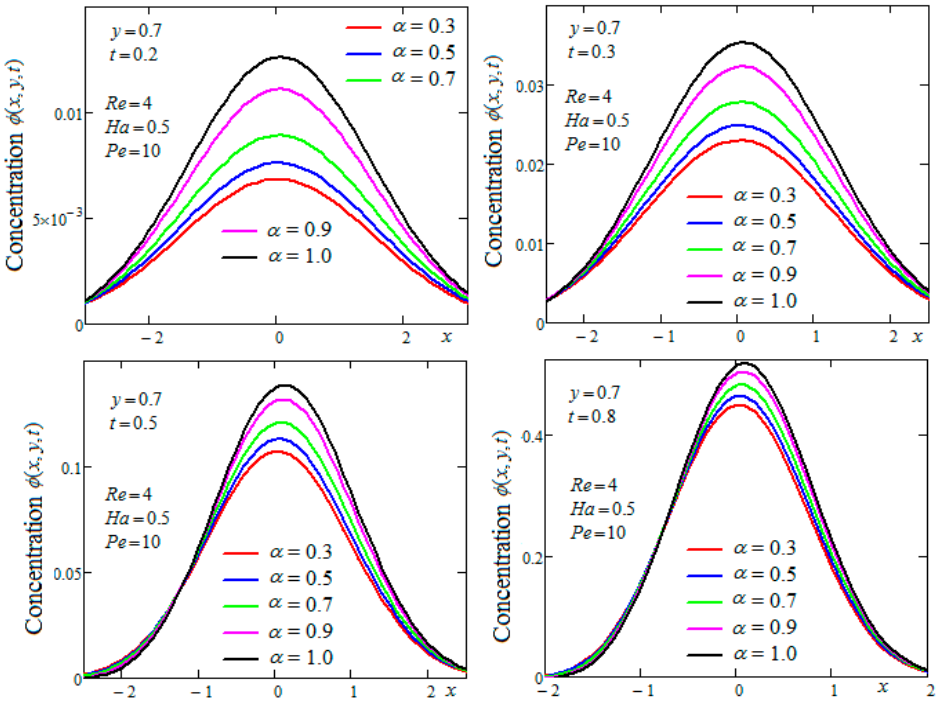

Figure 5. Profiles of the concentration $\phi(x, y, t)$ in the vertical position $y = 0.7$, for various values of the fractional parameter α and for different values of the time t.

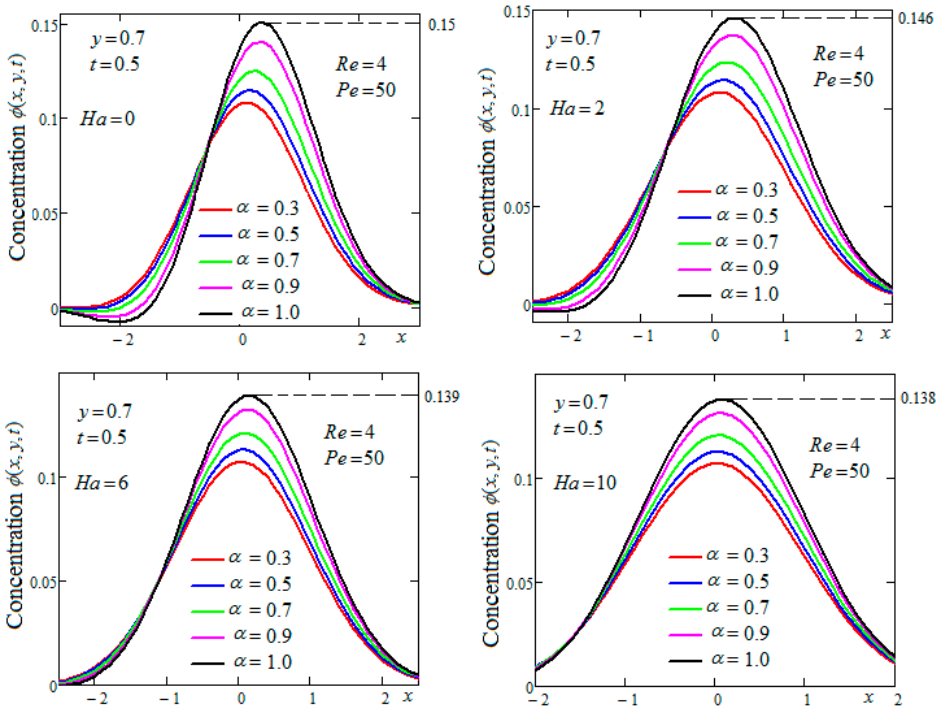

Figure 6. Profiles of the concentration $\phi(x, y, t)$ in the vertical position $y = 0.7$, for various values of the fractional parameter α and for different values of the Hartmann number Ha.

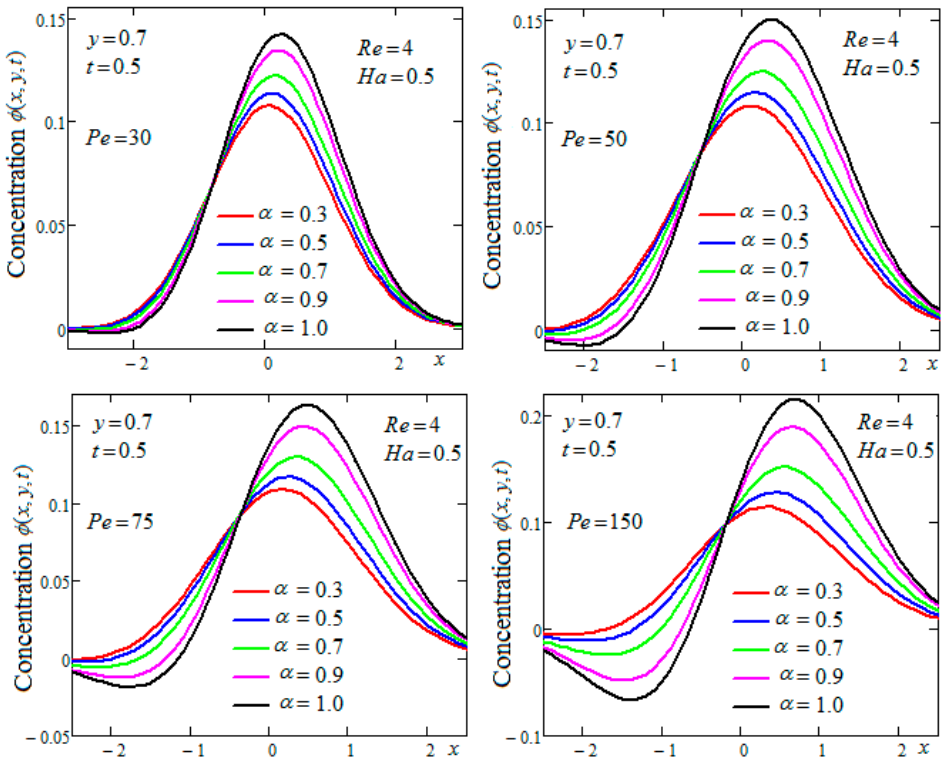

Figure 7. Profiles of the concentration $\phi(x, y, t)$ in the vertical position $y = 0.7$, for various values of the fractional parameter α and for different values of the Peclet number *Pe*.

Figure 4 presents the concentration distribution $\phi(x, y, t)$ of the tracers, versus x, at four vertical positions of the channel $y \in \{0.5, 0.6, 0.8, 1.0\}$, for fixed values of the Reynolds, Hartmann, and Peclet numbers and for five distinct values of the fractional parameter α. The concentration of the solute is increasing in relation to the variable y and reaches its maximum value in the middle of the range of variation in the longitudinal variable x. It is noted that the concentration values increase with regard to the fractional parameter α. It follows from here that for a diffusive process in which the mass flow is explained by a fractional constitutive equation, the solute concentration decreases at low values of the fractional memory parameter α.

The curves illustrated in Figure 5 highlight the fact that the concentration of the dissolved substance increases with the passage of time. On the other hand, let us note that the concentration of the solute decreases with the fractional parameter. This is because, for small values the fractional parameter α, the temperature gradient is more strongly influenced due to the kernel of the fractional derivative, so the generalized mass flux is reduced.

The curves in Figure 6 were drawn to highlight the impact of the magnetic field on the mass transfer. When the values of the magnetic parameter *Ha* boost, the values of the Lorentz force that slows the motion of the fluid increase, and therefore the intensity of the convection flow decreases. As a result, the values of the concentration of solutes decrease slightly with the increase in the values of the Hartmann number.

The impact of the Peclet number on the distribution of the pollutant in the flow channel is shown by the curves presented in Figure 7. Figure 7 illustrates how the solute concentration's absolute values increase with the increment of the Peclet number. This happens because the increase in the Peclet number values causes a rise in the advective transport rate, and therefore an increase in the solute concentration values.

6. Conclusions

The present paper analyzed the generalized transport phenomena of a solute in a magneto-hydrodynamic flow through a rectangular channel with permeable boundaries under the influence of an external magnetic field acting perpendicular to the flow direction.

The generalization consists of considering Fick's law, explained by a fractional differential equation with Caputo derivatives in relation to time. This model can describe more complicated mass diffusion processes.

An analytical method has been employed to resolve transport equations that depend on time. The analytical solution of the solute concentration is expressed with a confluent hypergeometric function and with the generalized G–Lorenzo–Hartley functions.

The influences of various transport characteristic parameters such as the fractional memory parameter and the Reynolds, Hartmann, and Peclet numbers on the solute transport are investigated by numerical simulations and graphical representations using Mathcad software.

The important conclusions of the present investigation are as follows:

The generalized fractional model can lead to a reduction in the concentration of the solute in the flow channel, and thus to an improvement in the spread of the pollutant in the flow stream. This fact is due to the modification of mass flux in Fick's generalized law. Changing the values for the fractional parameter has the effect of weaker or stronger damping of the concentration gradient, thus changing the transfer of the solute. The amplitude of the solute concentration decreases if the magnetic parameter Ha enhances. Increases in the Peclet number values leads to intensity in the advective transport rate, and therefore to an increase in the solute concentration values.

The results obtained may be useful for investigating the contamination of fluid media with different pollutants.

Also, the analytical solutions could be useful for verifying the accuracy of numerical methods applied to the problem under study.

In the future, the authors intend to study problems regarding the following:

1. The comparative study of dispersion processes based on different types of memory using different fractional-order derivative operators;
2. Dispersion problems with memory and non-stationary advection velocity.

Author Contributions: Conceptualization, N.A.S.; Methodology, K.M.; Software, D.V.; Validation, D.V.; Formal analysis, N.A.S.; Investigation, K.M.; Writing—original draft, N.A.S.; Writing—review and editing, D.V.; Supervision, D.V.; Project administration, K.M. All authors have read and agreed to the published version of the manuscript.

Funding: This work was supported and funded by the Deanship of Scientific Research at Imam Mohammad Ibn Saud Islamic University (IMSIU) (grant number IMSIU-DDRSP2603).

Data Availability Statement: The original contributions presented in this study are included in the article. Further inquiries can be directed to the corresponding author.

Acknowledgments: This work was supported and funded by the Deanship of Scientific Research at Imam Mohammad Ibn Saud Islamic University (IMSIU) (grant number IMSIU-DDRSP2603).

Conflicts of Interest: The authors declare no conflict of interest.

Nomenclature

U	Velocity
u	non-dimensional velocity
$C(X, Y, T)$	solute concentration

$\phi(x, y, t)$	non-dimensional concentration
$\vec{J}$	Diffusion flux
D	Uniform molecular diffusion
μ	Viscosity
ρ	Density
ν	Kinematic viscosity
$\vec{e}_X$	Unit vector of the X-axis
$\frac{\partial P}{\partial X}$	Pressure gradient in the flow direction
B_0	external magnetic field
Re	Reynolds number
Ha	Hartmann number
Pe	Peclet number
${}^{C}D_t^{\alpha}$	Caputo time-fractional derivative

References

1. Decker, D.L.; Tyler, S.W. Evaluation of flow and solute transport parameters for heap leach recovery materials. *J. Environ. Qual.* **1999**, *28*, 543–555. [CrossRef]
2. Sun, L.; Qiu, H.; Wu, C.; Niu, J.; Hu, B.X. A review of applications of fractional advection–dispersion equations for anomalous solute transport in surface and subsurface water. *WIREs Water* **2020**, *7*, e1448. [CrossRef]
3. Metzler, R.; Klafter, J. The restaurant at the end of the random walk: Recent developments in the description of anomalous transport by fractional dynamics. *J. Phys. A Math. Gen.* **2000**, *37*, R161–R208. [CrossRef]
4. Benson, D.A.; Wheatcraft, S.W.; Meerschaert, M.M. Application of a fractional advection-dispersion equation. *Water Resour. Res.* **2000**, *36*, 1403–1412. [CrossRef]
5. Povstenko, Y.Z. Fundamental solutions to time-fractional advection diffusion equation in a case of two space variables. *Math. Probl. Eng.* **2014**, *2014*, 705364. [CrossRef]
6. Jiang, W.; Lin, Y. Approximate solution of the fractional advection-dispersion equation. *Comput. Phys. Commun.* **2010**, *181*, 557–561. [CrossRef]
7. Nasrudin, F.S.M.; Phang, C.; Kanwal, A. Fractal-fractional advection-diffusion-reaction equations by Ritz approximation approach. *Open Phys.* **2023**, *21*, 20220221. [CrossRef]
8. Wang, F.; Li, Z.L.; Zhang, Y.; Guo, J. Fractional derivative modeling for sediment suspension in ice-covered channels. *Environ. Sci. Pollut. Res.* **2023**, *30*, 12508–12520. [CrossRef] [PubMed]
9. Qiao, C.; Xu, Y.; Zhao, W.; Qian, J.; Wu, Y.; Sun, H.G. Fractional derivative modeling on solute non-Fickian transport in a single vertical fracture. *Front. Phys.* **2020**, *8*, 378. [CrossRef]
10. Grant, J.; Wilkinson, M. Advection-diffusion equation with absorbing boundary. *J. Stat. Phys.* **2015**, *160*, 622–635. [CrossRef]
11. Wang, W.; Barkai, E. Fractional advection-diffusion-asymmetry equation. *Phys. Rev. Lett.* **2020**, *125*, 240606. [CrossRef] [PubMed]
12. Das, S.; Raut, S.; Mondal, K.K. Analyzing the effects of suction and injection Reynolds number on the transport process in a hydromagnetic flow through a channel of reactive porous walls. *Chin. J. Phys.* **2024**, *87*, 510–524. [CrossRef]
13. Hristov, J. Non-local kinetics: Revisiting and updates emphasizing fractional calculus applications. *Symmetry* **2023**, *15*, 632. [CrossRef]
14. Vieru, D.; Fetecau, C.; Ahmed, N.; Shah, N.A. A generalized kinetic model of the advection-dispersion process in a sorbing medium. *Math. Model. Nat. Phenom.* **2021**, *16*, 39. [CrossRef]
15. Kacur, J.; Keer, R.V. Solution of contaminant transport with adsorption in porous media by the method of characteristics. *Math. Model. Num. Anal.* **2001**, *35*, 981–1006. [CrossRef]
16. Hristov, J. The fading memory formalism with Mittag-Leffler-type kernels as a generator of non-local operators. *Appl. Sci.* **2023**, *13*, 3065. [CrossRef]
17. Tarasov, V.E.; Tarasova, S.S. Fractional Derivatives and Integrals: What Are They Needed For? *Mathematics* **2020**, *8*, 164. [CrossRef]
18. Diethelm, K. *The Analysis of Fractional Differential Equations. An Application-Oriented Exposition Using Differential Operators of Caputo Type*; Springer: Berlin/Heidelberg, Germany, 2010.
19. Tomovski, Z.; Sandev, T. Fractional wave equation with a frictional memory kernel of Mittag-Leffler type. *Appl. Math. Comput.* **2012**, *218*, 10022–10031. [CrossRef]
20. Gradstein, I.S.; Ryzhik, I.M. *Tables of Integrals, Sums, Series, and Products*; Academic Press: New York, NY, USA, 1965.
21. Abramowitz, M.; Stegun, I.A. (Eds.) Chapter 13: Confluent Hypergeometric Functions. In *Handbook of Mathematical Functions with Formulas, Graphs, and Mathematical Tables*, 9th ed.; Dover: New York, NY, USA, 1972; pp. 503–515.

22. Riley, K.F.; Hobson, M.P.; Bence, S.J. *Mathematical Methods for Physics and Engineering*, 3rd ed.; Cambridge University Press: Cambridge, UK, 2010; p. 455.
23. Vieru, D.; Zafar, A.A. Some Couette flows of a Maxwell fluid with wall slip condition. *Appl. Math. Inform. Sci.* **2013**, *7*, 209–219. [CrossRef]
24. Lorenzo, C.F.; Hartley, T.T. *NASA/TP-1999-209424/REV1, Generalized Functions for the Fractional Calculus*; The NASA STI Program Office, Glenn Research Center: Cleveland, OH, USA, 1999.

Disclaimer/Publisher's Note: The statements, opinions and data contained in all publications are solely those of the individual author(s) and contributor(s) and not of MDPI and/or the editor(s). MDPI and/or the editor(s) disclaim responsibility for any injury to people or property resulting from any ideas, methods, instructions or products referred to in the content.